Organic Process Research & Development

Article

pubs.acs.org/OPRD

Simultaneous API Particle Size Reduction and Polymorph Transformation Using High Shear

Ehrlic Lo,* Elias Mattas, Chenkou Wei, David Kacsur, and Chien-Kuang Chen

Bristol-Myers Squibb Company, Chemical Development, One Squibb Drive, New Brunswick, New Jersey 08903-0191, United States

ABSTRACT: This case-study outlines the development and scale-up of a novel solvent-mediated process for producing small crystals. The process combines polymorph transformation with high shear to produce API with a desirable crystal phase and morphology that meets the particle size acceptance criteria (d_{90} < 75 μm). The impact of process parameters was investigated, and suitable scaling parameters were identified. Subsequently, the process was successfully scaled up to generate 100 kg of the API of the target crystallographic form with the desired powder properties.

1. INTRODUCTION

One of the recent challenges in pharmaceutical development has been the increasing prevalence of oral drug candidates with limited aqueous solubility.[1,2] These compounds often demonstrate slow dissolution in biological fluids, resulting in insufficient systemic exposure and, consequently, suboptimal efficacy in patients. To address these issues, several approaches have been developed to improve the dissolution rates of poorly soluble drugs, e.g., particle size reduction via crystallization and mechanical processes, isolation of the API as an alternative salt form, prodrug, amorphous form, complex of higher solubility, or a self-emulsifying system.[3]

The dissolution rates of most drug candidates can be improved by reducing crystal size.[4,5] According to the Noyes−Whitney equation, the dissolution rate is directly dependent on increased surface area, achieved by a reduction in crystal size. One way to achieve controlled particle sizes is to carry out crystallization at high supersaturation, promoting a higher rate of nucleation as compared to less concentrated solutions. Through understanding of API solubility, the degree of supersaturation during batch crystallization can be controlled by adjusting the rate of cooling, the antisolvent composition and addition rate, the API concentration, or the chemical reaction conditions.[6,7] Controlling supersaturation in this way often provides control of crystal nucleation and growth rates and, hence, control of the final particle size distribution of the product. When in situ supersaturation control is not possible in typical batch crystallization processes, other techniques can be used. One such specialized approach to achieve uniformly high supersaturation for the generation of small particles is impinging jet crystallization.[8,9] This process, though elegant, requires an atypical setup and may generate undesired polymorphs due to extremely high supersaturation at the mixing zone.

Alternatively, particle size of solid API can be reduced postcrystallization by mechanical means. Particles can be milled to less than 50 μm via dry milling techniques such as pin milling or air attrition (jet) milling.[10] Dry milling efficiently reduces the particle size either through impact against the pins or surface or through particle−particle collisions. However, potential drawbacks of dry milling techniques include heat generation (pin milling) or compaction (jet), which could result in polymorphic transformations such as desolvation and/or loss of crystallinity. In addition, powders that have the propensity to bridge may not flow easily through the mill, the milling process may adversely affect powder properties,[11] and special containment facilities are often required to minimize worker exposure due to dust generation.

Another technique employed for particle size reduction of API is wet milling.[12] This process generally involves recirculating a slurry of the API through a high-shear source (wet mill), resulting in breakage of the crystallized particles to the desired particle size. This technique prevents dust generation but is dependent on particle morphology, crystallographic properties, and the desired final particle size, which may require long cycle times.

Another specialized technique involves generating secondary nucleation under high shear to achieve a small particle size distribution.[13] Here, a high-shear rotor−stator device is used for the controlled generation of fine particles via secondary nucleation under a relatively lower supersaturation than would be required in an exclusively batch operation.

Since many APIs can exist as different polymorphs, techniques to control specific polymorphic transformations have been developed.[14] These techniques are largely based on the differential stability of the respective polymorphs and use of temperature, additives, and solvent as the controlling parameters. Ultimately, the objective is to identify and select the most thermodynamically stable form and determine processing conditions to ensure its consistent manufacture.[15]

In this case study, we describe the development and scale-up of a novel method for producing small crystals during a solvent-mediated polymorphic transformation coupled with high shear provided by a rotor−stator.[16] This method reproducibly produces one of at least two polymorphs, converts a metastable form to the thermodynamically stable form, and simultaneously forms small particles under a high-shear environment.

Received: September 13, 2011
Published: December 5, 2011

ACS Publications © 2011 American Chemical Society

dx.doi.org/10.1021/op2002529 | *Org. Process Res. Dev.* 2012, 16, 102−108

2. CASE STUDY

Polymorph Selection. BMS-A, a potential treatment of prostate cancer,[17] is classified as a BCS Class II compound, having high permeability but low gastric solubility. During early polymorph screenings, a number of different polymorphs were identified for this compound (Table 1).

Table 1. Polymorphs of BMS-A

polymorph	structure	denoted as
neat	(BMS-A)	1
acetic acid solvate	(BMS-A) CH_3COOH	2
monohydrate hemiacetic acid solvate	(BMS-A) (H_2O) $(CH_3COOH)1/2$	3
hemihydrate	(BMS-A) $(H_2O)1/2$	4

While the neat form (Form 1) of the API was found to have better aqueous solubility (58 μg/mL) as well as enhanced oral exposure, it also had the propensity to transform to the hemihydrate (Form 4) upon exposure to moisture. Because the preferred formulation utilized a wet granulation process to minimize operator exposure during drug product formulation, the hemihydrate (Form 4) was selected for development as the final form in spite of the reduced solubility.

Due to the lower solubility of Form 4 (32.4 μg/mL), particle size was identified as a critical quality attribute for the drug substance to permit a faster dissolution rate based on the increased surface area. The initial acceptance criterion for the drug substance particle size distribution was established as d_{90} < 75 μm on the basis of drug product dissolution performance.

Initial Investigation. The exposure limit for BMS-A was established at <1 μg/m^3; therefore, mechanical milling was an undesired option for particle size reduction due to containment requirements to mitigate potential operator exposure during handling of the dry powder. Because of this constraint, solvent-mediated alternatives were investigated to produce BMS-A drug substance with the desired particle size.

A direct crystallization process was initially developed to produce Form 4 crystals of the desired particle size. Two streams, (1) BMS-A dissolved in acetic acid and (2) water (the antisolvent), were added cocurrently to the crystallizer. This process generated the desired hemihydrate polymorph with a d_{90} of approximately 20 μm, well below the target particle size limit of 75 μm. Figure 1 shows a micrograph of typical material, exhibiting a columnar crystal habit, isolated from this process.

The columnar crystal habit of the material generated in this process led to a number of downstream processing issues. First, the isolation of these columnar crystals required extended filtration and drying times. Second, and perhaps the more significant issue, was the propensity of these crystals to agglomerate, both during the crystallization and during agitated drying. These agglomerates retarded the dissolution of the API during formulation studies, necessitating an additional, potentially dusty, delumping operation via a CoMil unit to break the majority of the large agglomerates. Given the low exposure limits for this compound, development of an alternate API process became necessary.

On the basis of the propensity of the compound to readily form agglomerates with the initial process, a solvent-mediated polymorph transformation process was evaluated as an alternative to the direct crystallization process.

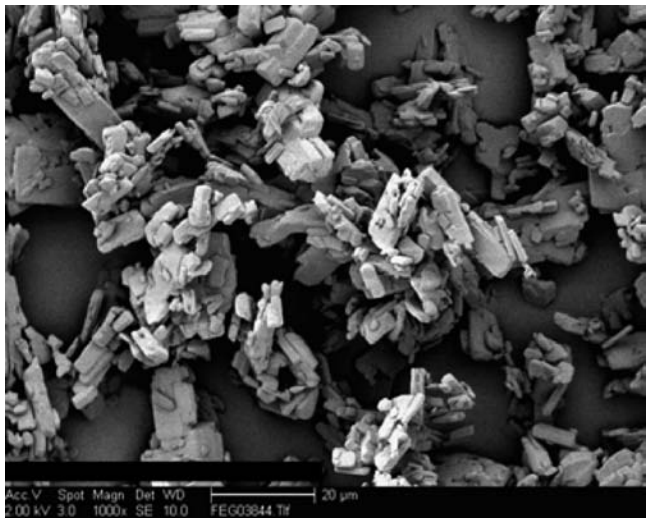

Figure 1. Optical image of columnar BMS-A (Form 4) isolated from semibatch crystallization.

Table 2 illustrates the thermodynamic stabilities of each of these polymorphs of BMS-A. The monohydrate hemiacetic acid solvate (Form 3) is thermodynamically favored in solutions containing <79.6 vol% water in acetic acid, with Form 4 preferred at higher concentrations of water.

Table 2. Stability of key polymorphs of BMS-A in different water−acetic acid ranges

stable polymorph	water−acetic acid mixture at 25 °C (water vol %)
(BMS-A) CH_3COOH (Form 2)	0.0
(BMS-A) (H_2O) $(CH_3COOH)1/2$ (Form 3)	0.0−79.6
(BMS-A) $(H_2O)1/2$ (Form 4)	79.6−100

Formation of Form 3 was achieved by the addition of water to a 20 wt % solution of BMS-A dissolved in acetic acid. Several experiments evaluated the impact of processing conditions on the rate of solvent-mediated transformation from Form 3 to Form 4. To facilitate this experimental work, an inline Raman method was developed to monitor the polymorph transformation process. Adding water beyond 79.6 vol% and holding the slurry for more than 30 h resulted in a slow transformation of Form 3 to the desired Form 4. The rate of this conversion was significantly enhanced by heating the Form 3 slurry to 50 °C, which completed the transformation within 30 min (Figure 2) as monitored by Raman. Powder X-ray diffraction (pXRD) (Figure 3) was used to confirm the generation of the desired form, and the particles generated from this process were analyzed by scanning electron microscope (SEM) (Figure 4) and by Malvern laser diffraction.

As opposed to the columnar-like morphology observed in the direct crystallization process, this polymorph-transformation process afforded a tabular crystal habit. This serendipitous outcome was desirable from a downstream processing perspective, given the likely improved filtration and drying rates and the potential reduction in agglomeration. However, the lack of particle size control remained a serious drawback, as can be seen by the wide distribution in particle size in Figure 4.

A number of batches were produced using this form-transformation process on 5−10 g scale. In each batch the

dx.doi.org/10.1021/op2002529 | Org. ProcessRes. Dev. 2012, 16, 102−108

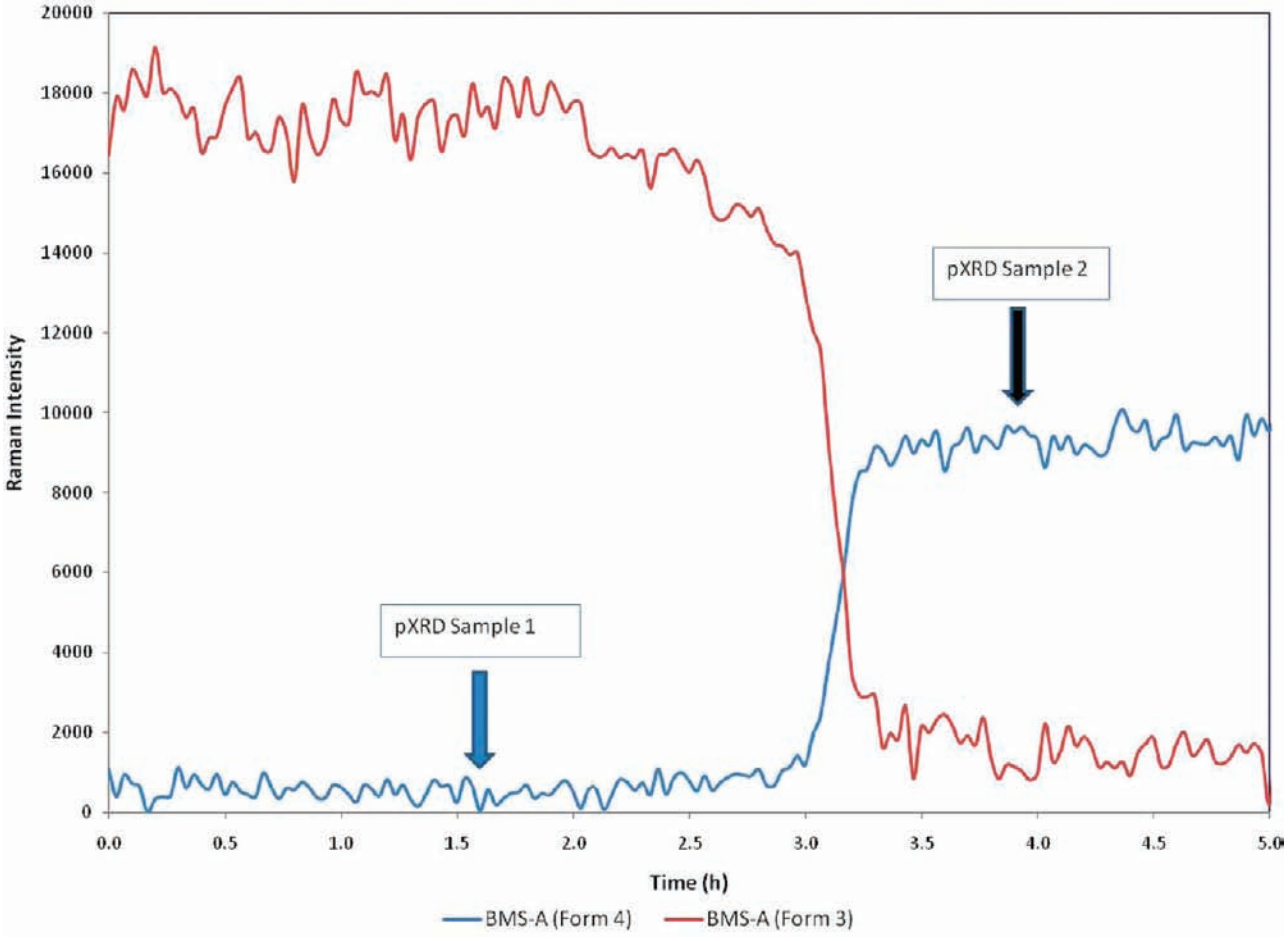

Figure 2. Raman profile of polymorph transformation at 50 °C.

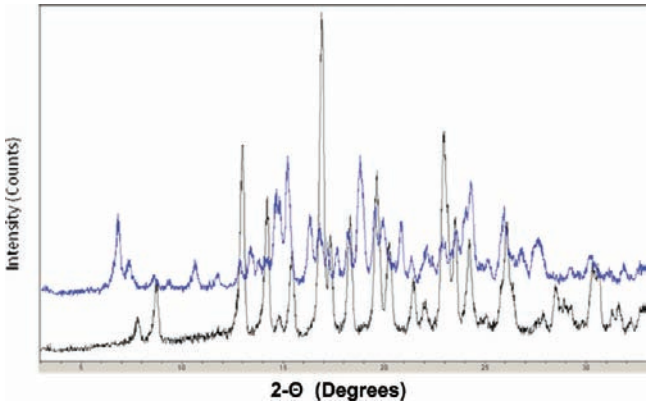

Figure 3. pXRD pattern of Form 3 (blue) and Form 4 (black).

Form 3 slurry was held at 50−55 °C under similar concentrations. The transformations for the three batches occurred within 4 h of reaching the desired temperature; however, in the absence of additional controls, inconsistent particle size distributions were realized (Figure 5). The particle size distributions were relatively polydisperse, with d_{90}/d_{10} ranging between 4.7 and 7.0, with a d_{90} exceeding 150 μm for one batch.

Particle Size Control Process Development. Subsequent process development efforts focused on modifying the aforementioned process to control particle size by conducting the polymorph transformation in a high-shear environment by

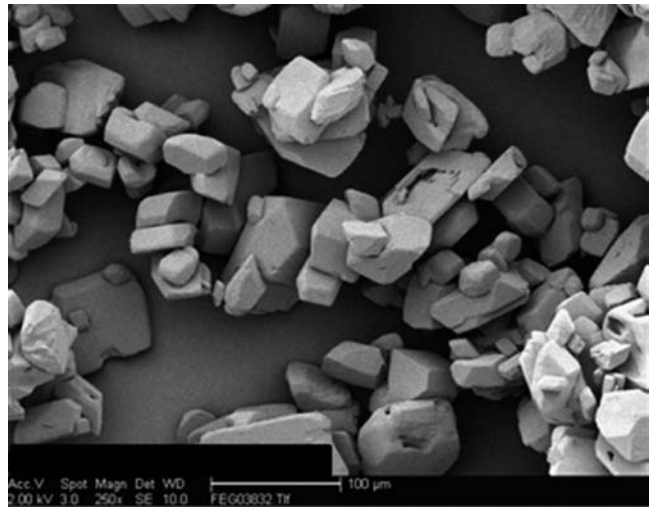

Figure 4. SEM of BMS-A with tabular morphology (Form 4).

applying rotor−stator technology.[16] It was hypothesized that imparting shear during the transformation would result in enhanced control of the particle size through two possible mechanisms. One possible mechanism is that in the solvent-mediated phase transformation, a suspension of a metastable phase gradually dissolves, which generates supersaturation with respect to the stable phase, resulting in nucleation and growth of the stable phase. Since nucleation, either surface nucleation

dx.doi.org/10.1021/op2002529 | Org. ProcessRes. Dev. 2012, 16, 102−108

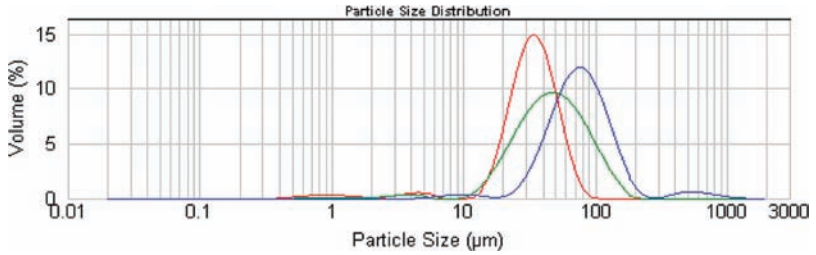

Figure 5. Particle size distribution overlays of different batches of tabular BMS-A.

or secondary nucleation,[18] is involved, its rate can be increased significantly in a high-shear environment, e.g. in a rotor−stator. With a significantly increased number of nuclei, the growth of individual crystals is inhibited, and the resultant particle size will be small. The second possible mechanism is within the solid-state transformation scenario; due to a change in crystal structure, the crystals may break or crack to afford the desired polymorph with a reduced particle size.[19,20] It is conceivable that high-shear stress will facilitate this process of crystal breakage.

Methods. A series of optimization experiments run on 25-g scale were performed in a jacketed 1-L Chemglass reactor with overhead stirring and bottom valve. Two in situ analytical probes were inserted into the reactor: in-line Raman and focused-beam reflectance microscopy (FBRM) and a recycle loop slip-stream contained an inline IKA Works UTL-25 Turrax wet mill. The Raman spectroscopic probe (Kaiser Optical Systems, optical fiber) has a typical laser power of 150−200 mW at 785 nm with exposure time for the measurement set at 10 s with 10 accumulations. The method monitored a peak shift from 1438 cm^{-1} (Form 3) to 1430 cm^{-1} (Form 4). The FBRM probe (Lasentec, model D600L) allowed for chord lengths to be measured with a 25−250 μm range with exposure time set at 15 s. These two probes allowed for determining over time the properties of the solid phase. The form of the crystals and chord length distribution were tracked with respect to time.

This experimental work led to a process where Form 3 was produced by a semibatch process through the addition of water to a 20 wt % solution of API in acetic acid to afford a final ratio of 4.25:1 H_2O:HOAc. After the completion of the water charge, the material was pumped through the recirculation loop with an inline wet mill serving as the high-shear source. The UTL-25 uses rotor−stator technology and a schematic demonstrating the principle of operation is shown in Figure 6. The differential speed between the rotor and the stator imparts extremely high shear and turbulent energy in the gap between the rotor and stator.

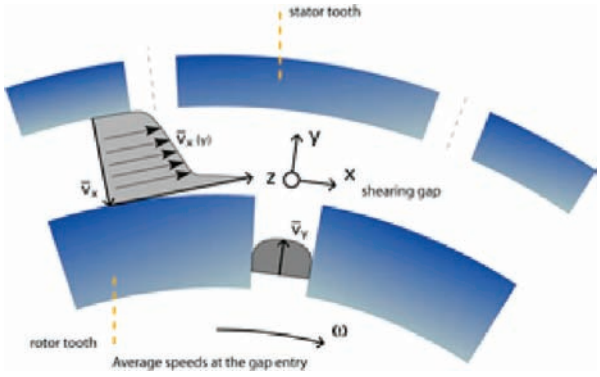

Figure 6. Schematic of rotor−stator high-shear mixing environment[21].

During the recirculation through this high-shear zone, the batch was slowly heated to 50 °C to promote the polymorph transformation. The batch was held at 50 °C with continuous recirculation and the process was monitored using Raman and FBRM.

The inline Raman was used to determine the completion of the polymorph transformation, and the FBRM was used to confirm that there was a decrease in the c_{90} particle size coupled with an increase in the total counts during the transformation process. In addition, the polymorph transformation was confirmed by pXRD and the final particles were inspected using optical microscopy and SEM measurements to ensure the desired crystallographic form and particle size were achieved. The API generated by this process was consistently of the tabular habit and within the target particle size distribution of d_{90} < 75 μm. Figure 7 plots the PAT measurements during a typical polymorph transformation, and Figure 8 shows the change in morphology of the crystal during the polymorph transformation via optical microscopy.

3. PROCESS DESIGN CONSIDERATIONS

The degree of shear imparted to material passing through the rotor−stator arrangement is determined by the speed of rotation and the number of rotor−stator elements present. For scale-up purposes and ease of comparison, tip speed, shear rate, and shear frequency are often used to characterize these systems.[12] The tip speed is simply the linear velocity at the radius of the outermost rotor and is expressed as follows:

$$\text{tip speed, } V = \pi \cdot n \cdot D$$

where: n = rotor rotational speed (rev/s) and D = rotor diameter (m)

The shear rate is the velocity of the fluid over the cross-sectional gap between the rotor and stator and is expressed as follows:

$$\text{shear rate, } \tau = V/g$$

where V = tip speed of rotor (m/s) and g = gap distance (m)

The shear frequency can be characterized as the number of occurrences that the rotor and stator openings mesh. It allows for different rotor−stator configurations to be compared on a normalized basis. Using the tip speed alone, information on the mill configuration is lost. The shear frequency is expressed as follows:

dx.doi.org/10.1021/op2002529 | Org. ProcessRes. Dev. 2012, 16, 102−108

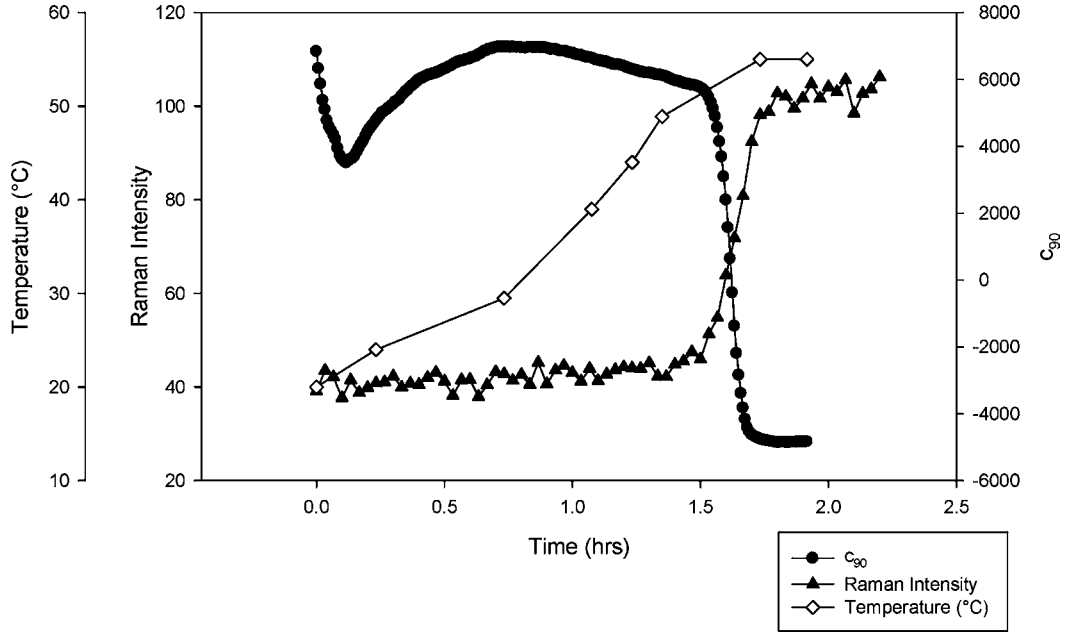

Figure 7. Raman and Lasentec trend overlay for a transformation.

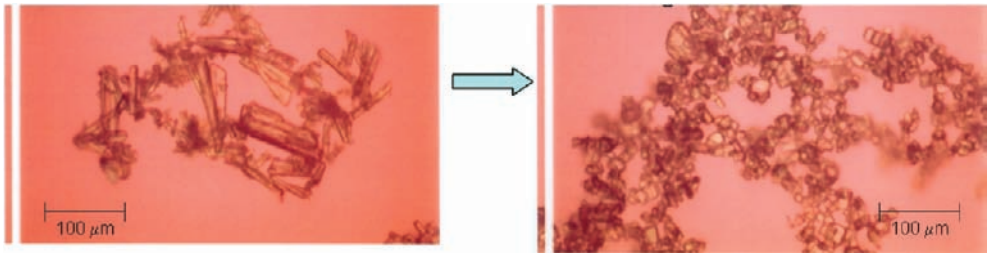

Figure 8. Optical microscopy images of Form 3 (left) and Form 4 (right).

Table 3. Turrax operating conditions and performance

parameters	batch 1	batch 2	batch 3	batch 4	batch 5	lab batch
rotor–stator (LaborPilot DR-2000/4)	not used	two-stage coarse	two-stage coarse	two-stage coarse	two-stage fine	one-stage fine (UTL-25)
tip speed (m/s)	N/A	9	12.5	23	23	9
shear rate (1/s)	N/A	36000	46535	94300	94300	17907
shear frequency (1/s)	N/A	3020	3900	7800	143000	15200
turnover time (min)	N/A	12	10	10	12	7
slurry flow rate (LPM)	N/A	1.8	2.1	2.1	1.8	0.075
d_{10} (μm)	55.9	49.4	40	25.1	19.8	15.8
d_{50} (μm)	96.5	86.7	67.4	46.9	35.8	34.8
d_{90} (μm)	167.2	146.1	111.2	83.7	73.8	70.8
polydispersity index (d_{90}/d_{10})	3	3	2.8	3.3	3.7	4.5
transformation time (h)	6	1	1	0.75	0.75	0.75

$$\text{shear frequency (fs) [=] 1/s [=] Hz: fs} = \sum_{1}^{\#\text{of generators}} \sum_{1}^{\#\text{of rows}} (\#\text{of teeth}_{\text{rotor}} \times \#\text{of teeth}_{\text{stator}}) \times n$$

To further study the impact of process conditions and identify potential scale-up effects of the polymorph transformation, a series of batches were executed on a 1.3-kg scale using a larger IKA Works LaborPilot DR 2000/4. Parameters for the operation of the LaborPilot DR 2000/4, such as shear rate, shear frequency, and turnover time across the five batches are compared to those for the smaller IKA Works UTL-25 Turrax in Table 3.

Within the limited range studied, the turnover time did not seem to impact the particle size significantly. The tip speed, shear rate, and shear frequency appeared to impact the final particle size distribution of the final product. At shear frequencies below 7800 s^{-1} and tip speeds below 23 m/s, the particle size decreases monotonically; however, at shear frequencies above 7800 s^{-1}, there is a diminishing effect on the final PSD, and further particle size reduction is not achieved, as seen in Figure 9.

A number of other process parameters were varied to more completely define the design space for the process.

dx.doi.org/10.1021/op2002529 | Org. ProcessRes. Dev. 2012, 16, 102–108

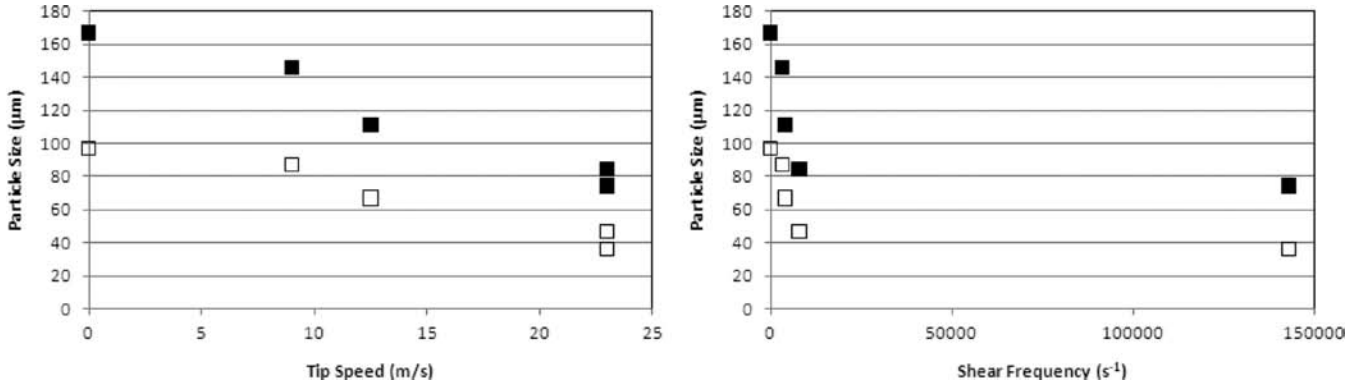

Figure 9. Relationship between BMS-A particle size and shear parameters on kilo-lab scale, d_{90} (□) and d_{50} (■) are shown.

Table 4. Pilot-plant Turrax operating conditions

parameters	desired operating condition	actual operating range
tip speed (m/s)	23	23
shear rate (1/s)	46,000	46,000
shear frequency (1/s)	258,000	258,000
turnover time (min)	6.7	5–6.9
slurry flow rate (L/min)	120	118–123

Concentration of the substrate, 15–27.5 wt %, and the ratio of water to acetic acid, 4–1 through 8–1, did not impact the final API particle size. In addition, the number of batch turnovers and the turnover times, ranging between 5–12 min, did not have a significant impact. It was found that the operating temperature was found to impact the resulting particle size distribution.

The temperature ramp rate and the final holding temperature for the polymorph transformation were studied. At ramp rates between 0.25 °C/min and 1 °C/min (from 20 to 50 °C), there was no significant difference in the final particle size. The temperature at which the polymorph transformation occurred, however, appeared to have significant effect on the resulting particle size distribution. The resulting particle size was minimized by operating between 45 and 50 °C, and the particle size increased outside of this window. The operating window was constrained accordingly in order to achieve consistently small particles. A possible explanation for the increase in particle size observed outside the 45–50 °C window could be attributed to the dominance of growth over the nucleation in these two regimes resulting from two different phenomena. It is believed that at higher temperatures (>50 °C), the solubility of Form 4 relative to Form 3 is decreased, potentially reducing the rate of secondary nucleation. In addition, at higher temperatures, given the increased solubility of Form 4, supersaturation is decreased, also resulting in a reduction in the rate of secondary nucleation. At lower temperatures the rate of form transformation may serve to limit supersaturation of the desired form, thus favoring growth as well.

Pilot-Plant Results. On the basis of the kilo-lab results, the operating limits for scale-up were set as follows: a shear frequency of at least 7800 s^{-1} and a tip speed of at least 23 m/s. The actual operating conditions are listed in Table 4. The high-shear polymorph transformation process was scaled to a 2000-L pilot-plant crystallizer using the three-stage IKA Works DRS2000/10 wet mill, with a pumping stage and two fine rotor–stators (Figure 10). The shear frequency produced with

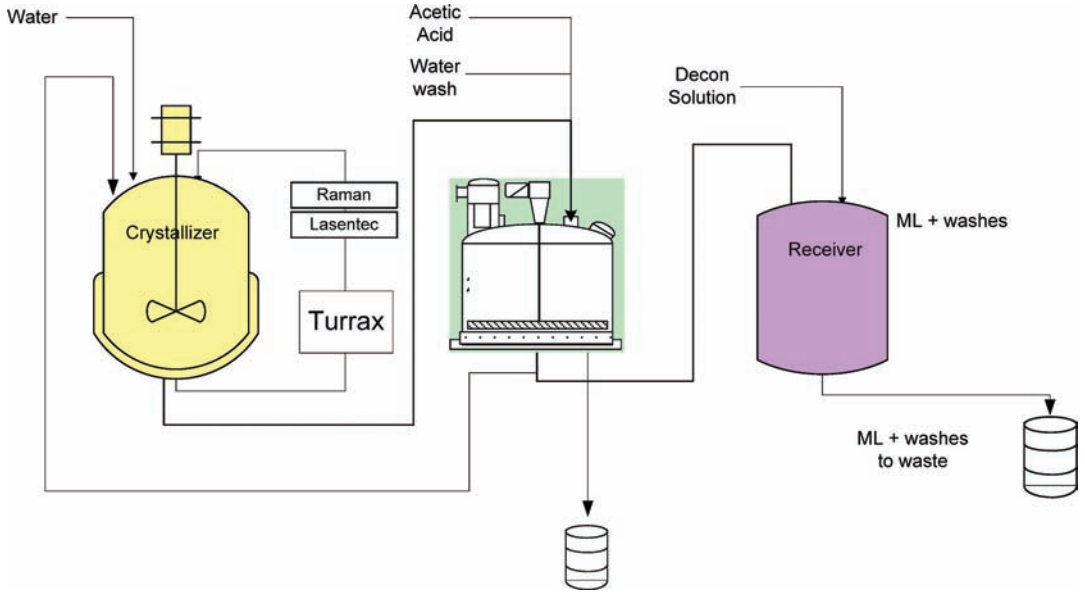

Figure 10. Schematic of pilot-plant equipment setup.

dx.doi.org/10.1021/op2002529 | Org. ProcessRes. Dev. 2012, 16, 102–108

this configuration was approximately 30 times higher than the 7800 s^{-1} minimum requirement defined during development. On the basis of the kilo-lab results (Figure 10), the higher shear frequency environment was not expected to cause any processing problems or particle attrition due to the observed flattening in the PSD curve at shear frequencies above 7800 s^{-1}.

The Raman profile indicated that the form change started shortly after the batch reached a temperature of 50 °C. Simultaneously, the Lasentec FBRM profile indicated a drop in the c_{90} particle size and a corresponding increase in the total particle counts, similar to the laboratory trends depicted in Figure 7.

Both batches produced the required hemihydrate polymorph of the tabular crystal habit, with a particle size d_{90} between 60 and 70 μm. The batches were isolated with filtration fluxes exceeding 3000 L/m^2 h, and improved drying rates as compared to those of the direct crystallization process. This process was successfully implemented in additional campaigns, producing hundreds of kilograms of acceptable quality API.

4. CONCLUSION

A relatively simple and novel method employing high shear has been developed for producing small crystals of the desired crystallographic form for a particular drug candidate. The process simultaneously controlled the form and particle size in a solvent-mediated polymorph transformation. This process avoids dry milling and has the potential to generate a range of particle size by tuning the process parameters of the crystallization and the high-shear operating conditions. Systematic experiments were carried out to explore the design space by identifying the process parameters that were critical to the quality of the final API. Tip speed and shear frequency were effective scaling parameters that allowed for effective generation of process understanding at laboratory scale. This understanding resulted in the rapid development of a robust process that was successfully scaled to 40-kg batches in our pilot plant.

In addition, this technology has successfully been applied to two other projects within the Bristol-Myers Squibb portfolio. This process can likely be applied to any polymorph transformation system that requires particle size control.

AUTHOR INFORMATION

Corresponding Author

ehrlic.lo@bms.com.

ACKNOWLEDGMENTS

We acknowledge the contributions of Jianji Wang, Venkatramana Rao, Mario Hubert, San Kiang, Srinivas Tummala, Jean Tom, Robert Waltermire, Frank Mastellone, Jeffrey Reinhardt, Matthew Casey, and Mariano Massari to the work.

REFERENCES

(1) Lipinski, C. A. *Am. Pharm. Rev.* **2002**, *5* (3), 82–85.
(2) Blagden, N.; de Matas, M.; Gavan, P. T.; York, P. *Adv. Drug Delivery Rev.* **2007**, *59*, 617–630.
(3) Mehta, S. C. *Bull. Tech. Gattefosse* **1998**, *91*, 65–72.
(4) Johnson, K.; Swindell, A. *Pharm. Res.* **1996**, *13* (12), 1796–1798.
(5) Hintz, R.; Johnson, K. *Int. J. Pharm.* **1989**, *51*, 9–17.
(6) Myerson, A., Ed. *Handbook of Industrial Crystallization*, 2nd ed.; Butterworth-Heinemann: Woburn, MA, 2002.
(7) Kim, S.; Lotz, B.; Lindrud, M.; Girard, K.; Moore, T.; Nagarajan, K.; Alvarez, M.; Lee, T.; Nikfar, F.; Davidovich, M.; Srivastava, S.; Kiang, S. *Org. Process Res. Dev.* **2005**, *9*, 894–901.
(8) Midler, M.; Paul, E. L.; Whittington, E. F.; Futran, M.; Liu, P. D.; Hsu, J.; Pan, S. H. Crystallization Method to Improve Crystal Structure and Size. U.S. Patent 5,314,506, 1994.
(9) Pesti, J.; Chen, C. K.; Spangler, L.; DelMonte, A.; Benoit, S.; Berglund, D.; Bien, J.; Brodfuehrer, P.; Chan, Y.; Corbett, E.; Costello, C.; DeMena, P.; Discordia, R.; Doubleday, W.; Gao, Z.; Gingras, S.; Gross, J.; Haas, O.; Kacsur, D.; Lai, C.; Leung, S.; Miller, M.; Muslehiddinoglu, J.; Nguyen, N.; Qiu, J.; Olzog, M.; Reiff, E.; Thoraval, D.; Totlebon, M.; Vanyo, D.; Vemishetti, P.; Wasylyk, J.; Wei, C. *Org. Process Res. Dev.* **2009**, *13* (4), 716–728.
(10) Nakach, M.; Authelin, J. R.; Chamayou, A.; Dodds, J. *Int. J Miner. Process.* **2004**, *74*, S173–S181.
(11) Rasenack, N.; Muller, B. N. *Pharm. Dev. Technol.* **2004**, *9* (1), 1–13.
(12) Lee, I.; Variankaval, N.; Lindemann, C.; Starbuck, C. *Am. Pharm. Rev.* **2004**, *7* (5), 120–128.
(13) Kamahara, T.; Takasuga, M.; Tung, H. H.; Hanaki, K.; Fukunaka, T.; Izzo, B.; Nakada, J.; Yabuki, Y.; Kato, Y. *Org. Process Res. Dev.* **2007**, *11* (4), 699–703.
(14) Kitamura, M. *J. Cryst. Growth* **2002**, *237–239*, 2205–2214.
(15) Karpinski, P. H. *Chem. Eng. Technol.* **2006**, *29* (2), 233–237.
(16) Wei, C.; Yang, B. Crystallization via High-shear Transformation, U.S. Pat. Appl. Publ., 2006160841, 2006.
(17) Xiao, H-Y; Balog, A.; Attar, R.; Fairfax, D.; Fleming, L.; Holst, C.; Martin, G.; Rossiter, L.; Chen, J.; Cvjic, M.-E.; Dell-John, J.; Geng, J.; Gottardis, M.; Han, W.-C.; Nation, A.; Obermeier, M.; Rizzo, C.; Schweizer, L.; Spires, T. Jr.; Shan, W.; Gavai, A.; Salvati, M.; Vite, G. *Bioorg. Med. Chem. Lett.* **2010**, *20* (15), 4491–4495.
(18) Ferrari, E. S.; Davey, R. *Cryst. Growth Des.* **2004**, *4* (5), 1061–1068.
(19) Yamanobe-Hada, M.; Ito, A.; Shindo, H. *J. Cryst. Growth* **2005**, *275* (1–2), e1739–e1743.
(20) Griesser, U. J. The Importance of Solvates. In *Polymorphism: In the Pharmaceutical Industry*; Hilfiker, R., Ed.; Wiley-VCH Verlag: New York, 2006; pp 222–224.
(21) *IKA-Works. IKA process technology* [Brochure]. Retrieved 12-June 2011 from http://www.ikaprocess.com/pdf/Process-Technology.pdf.